Electronic Supplementary Information (ESI)

Pressure-induced Dehydrogenative Coupling of Methane to Ethane by Platinum-loaded Gallium Oxide Photocatalyst

Fumiaki Amano,[1,2,]* *Chiho Akamoto,*[1] *Mizuki Ishimaru,*[1] *Satoshi Inagaki,*[2,3]*and Hisao Yoshida* [4,5]

[1] Department of Chemical and Environmental Engineering, The University of Kitakyushu, 1-1 Hibikino, Wakamatsu-ku, Kitakyushu, Fukuoka 808-0135, Japan.

[2] Precursory Research for Embryonic Science and Technology (PRESTO), Japan Science and Technology Agency (JST), 4-1-8 Honcho, Kawaguchi, Saitama 332-0012, Japan.

[3] Division of Materials Science and Chemical Engineering, Yokohama National University, 79-5 Tokiwadai, Hodogaya-ku, Yokohama 240-8501, Japan.

[4] Graduate School of Human and Environmental Studies, Kyoto University, Yoshida-nihonmatsu-cho, Sakyo-ku, Kyoto 606-8501, Japan.

[5] Elements Strategy Initiative for Catalysts and Batteries (ESICB), Kyoto University, Kyotodaigaku-Katsura, Nishikyo-ku, Kyoto 615-8520, Japan.

* E-mail: amano@kitakyu-u.ac.jp

1. Experimental details

1.1 Preparation of photocatalysts

TiO_2 ST-01 and TiO_2 P 25 were supplied from Ishihara Sangyo (Japan) and Nippon Aerosil (Japan), respectively. Y_2O_3, Nb_2O_5, Ta_2O_5, WO_3, ZnO, Ga_2O_3, GeO_2, and SnO_2 were purchased from Kojundo Chemical Laboratory (Japan). ZrO_2 and In_2O_3 were purchased from Wako Pure Chemicals (Japan). Hydrogen hexachloroplatinate(IV) hexahydrate (H_2PtCl_6•$6H_2O$) and tetraamineplatinum(II) chloride monohydrate ($Pt(NH_3)_4Cl_2$•H_2O) were purchased from Kanto Chemical (Japan).

Platinum cocatalyst was loaded on the oxide powder using an incipient wetness impregnation (IWI) method. The IWI is a conventional method to prepare highly dispersed metal-supported catalysts using a capillary action process. The powder (1.5 g) was mixed with an aqueous solution of H_2PtCl_6 (8.5 mmol L^{-1}, 900 μL, 0.1 wt% as Pt) and dried at 100 °C for 1 h. All of the supplied H_2PtCl_6 is deposited on the Ga_2O_3 surface after the evaporation to dryness. During photocatalytic reactions, the adsorbed Pt^{4+} species is quickly reduced to Pt^0 by photoexcited electrons since it is a strong electron acceptor ($PtCl_6^{2-} + 4e^- \rightarrow Pt + 6Cl^-$ E = 0.74 V vs. SHE). Therefore, Pt loaded metal oxide such as Pt/Ga_2O_3 can be formed under the photocatalytic reaction conditions. We also tested $Pt(NH_3)_4Cl_2$ as a precursor for Pt cocatalyst. Pt^{2+} is also easily reduced by photoexcited electrons ($Pt^{2+} + 2e^- \rightarrow Pt$ E = 1.19 V vs. SHE). The in-situ formation of Pt metal is guaranteed by the continuous H_2 evolution under photoirradiation.

1.2 Photocatalytic reaction

The photocatalyst powder (50 mg) was coated on a square area (5 cm × 5 cm) of a glass plate using water and dried at room temperature. The photocatalyst coated on the glass substrate was installed in a home-made stainless-steel reactor with a quartz window (5 cm × 5 cm). The distance between the glass substrate and the quartz window is about 0.25 mm, which is the thickness of a rubber gasket. The feed gas was ultra-high purity CH_4 (99.9995%) and Ar (> 99.995%). The total flow rate was controlled to 20 mL min^{-1} by mass flow controllers. Water vapor was introduced through a bubbler filled with deionized water at 25 °C. The pressure of water vapor was obtained from the dew point measured by a humidity transmitter (EE33, E+E Elektronik, Austria). A back-pressure valve was used to regulate the total pressure higher than 1 atm.

The light source was a 40-W low-pressure mercury lamp (wavelength 254 nm, Asumi Giken, Japan). The irradiance was measured by an optical power meter with a sensor for low-pressure mercury lamps (C9536 and H9535-254, Hamamatsu Photonics, Japan). The temperature of the reactor was cooled to 25 °C by a thermoelectric cooling device. The reactants and products were analyzed by online GC-8A gas chromatographs (Shimadzu, Japan) equipped with a thermal conductivity detector (TCD) and a flame ionization detector (FID). The column of MS-5A, Shincarbon ST, and Porapak-Q was used with a carrier of He, Ar, and N_2, respectively. The gas from the outlet was collected by GS5100 automatic gas samplers (GL Sciences, Japan).

1.3 Characterization

X-ray diffraction (XRD) measurement was carried out on a SmartLab diffractometer (Rigaku, Japan) using Cu Kα radiation. Scanning electron microscope (SEM) image was taken on JSM-7800F (JEOL, Japan). Transmission electron microscope (TEM) image was taken on JEM-3010 (JEOL, Japan) at 200 kV. Nitrogen adsorption isotherm was measured at −196 °C using a BELSORP-mini (Bel Japan, Japan) after evacuation at 200 °C for 2 h. Diffuse reflectance UV-

Vis spectrum was recorded on a UV-2600 spectrometer (Shimadzu, Japan) with an integrating sphere by using $BaSO_4$ powder as a reference. Thermogravimetry–differential thermal analysis (TG–DTA) was performed under air at a heating rate of 10 °C min^{-1} using a Thermo plus TG8120 (Rigaku, Japan).

Electron spin resonance (ESR) spectrum was recorded on JES-FA200 (JEOL, Japan). The sample powder (200 mg) was pre-evacuated at 25 °C or 200 °C for 30 min. The measurement was performed by soaking the sample tube in liquid nitrogen (−196 °C). The sample was irradiated by UV light emitted from a 300-W xenon lamp (Asahi Spectra, Japan) with a bandpass filter (center wavelength 248 nm).

Table S1. Physical properties of metal oxide samples

Sample	Supplier	Purity	Crystal system	Crystalline diameter [c] (nm)	XRD peak [d]
Y_2O_3	Kojundo [a]	0.9999	Cubic	49	(222)
TiO_2 (ST-01)	Ishihara Sangyo	—	Tetragonal (Anatase)	8	Anatase (101)
TiO_2 (P 25)	Nippon Aerosil	—	Tetragonal (Anatase, Rutile)	22	Anatase (101)
ZrO_2	Wako [b]	0.98	Monoclinic	45	(−111)
Nb_2O_5	Kojundo [a]	0.9999	Monoclinic	95	(110)
Ta_2O_5	Kojundo [a]	0.999	Orthorhombic	279	(001)
WO_3	Kojundo [a]	0.9999	Monoclinic, triclinic	113	(002)
ZnO	Kojundo [a]	0.9999	Hexagonal (Zincite)	190	(100)
Ga_2O_3	Kojundo [a]	0.999	Monoclinic (β-Ga_2O_3)	34	(002)
In_2O_3	Wako [b]	0.999	Cubic	55	(222)
GeO_2	Kojundo [a]	0.999997	Hexagonal	58	(101)
SnO_2	Kojundo [a]	0.9999	Tetragonal	35	(110)

[a] Kojundo Chemical Laboratory

[b] Wako Pure Chemical

[c] Crystalline diameter was estimated from the full width at the half-maximum (FWHM) of the XRD peak by using the Scherrer equation.

[d] Crystal lattice plane of the XRD peak for analysis of the crystalline diameter.

Table S2. BET specific surface area (S_{BET}), average particle size ($2r$), optical band gap (E_g), electronegativity (X), and conduction band minimum (E_{CB}) of metal oxide samples.

Sample	S_{BET} [a] ($m^2\ g^{-1}$)	$2r$ [b] (nm)	E_g [c] (eV)	X [d] (eV)	E_{CB} [e] (V vs. SHE)
Y_2O_3	12.9	92	5.55	5.39	−1.82
TiO_2 (ST-01)	302.3	5	3.23	5.81	−0.24
TiO_2 (P 25)	50.7	30	3.05	5.81	−0.15
ZrO_2	9.6	107	5.07	5.85	−1.12
Nb_2O_5	2.4	559	3.07	6.21	0.24
Ta_2O_5	1.7	388	3.85	6.26	−0.10
WO_3	4.3	194	2.66	6.57	0.80
ZnO	3.4	309	3.21	5.95	−0.09
Ga_2O_3	10.4	97	4.56	5.36	−1.36
In_2O_3	2.7	311	2.73	5.25	−0.56
GeO_2	1.9	724	5.93	6.38	−1.03
SnO_2	11.0	78	2.69	6.22	0.43

[a] S_{BET} was determined from the N_2 adsorption isotherm.

[b] The average particle size was calculated from S_{BET} and the density (ρ) of the main crystalline component in the oxide powder, hypothetically assuming that the particles are spherical with radius (r).

$$2r = \frac{6}{S_{\mathrm{BET}} \times \rho} \tag{1}$$

[c] E_g was determined from the diffuse reflectance UV-visible spectra.

[d] The X of metal oxide was obtained from the geometric mean of Mulliken's electronegativity of a neutral atom, which is the arithmetic mean of the electron affinity and the first ionization energy.

[e] E_{CB} was estimated from the equation, $E_{\mathrm{CB}} = -4.44 + X - 0.5\ E_g$.

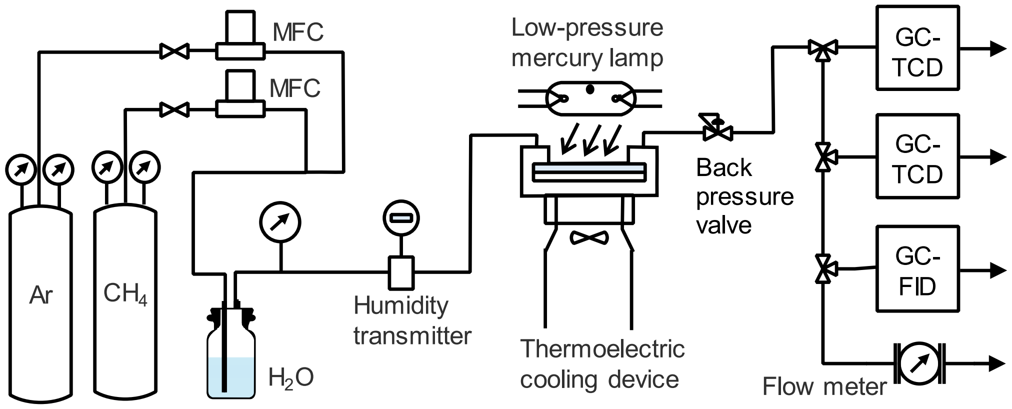

Figure S1. Schematic diagram of the experimental apparatus for the photocatalytic reaction.

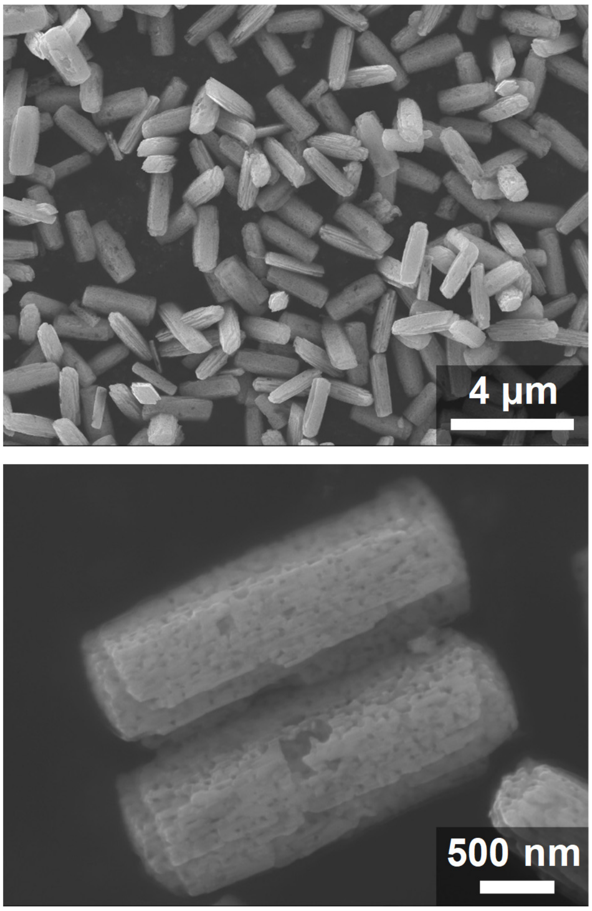

Figure S2. SEM images of Ga_2O_3 powder (99.99%, Kojundo Chemical Laboratory).

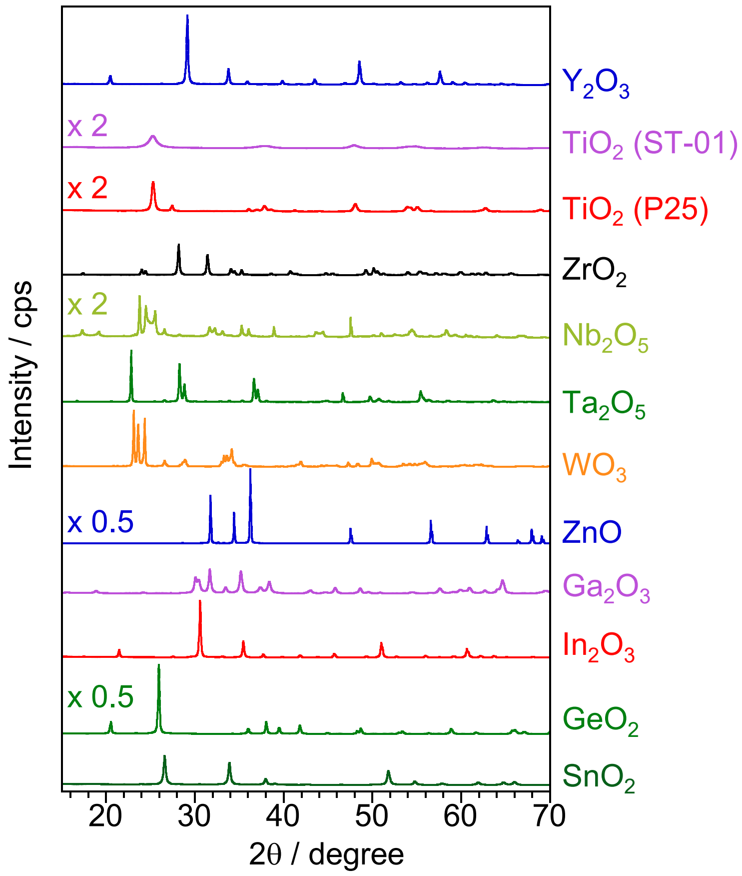

Figure S3. XRD patterns of the commercial metal oxide powders.

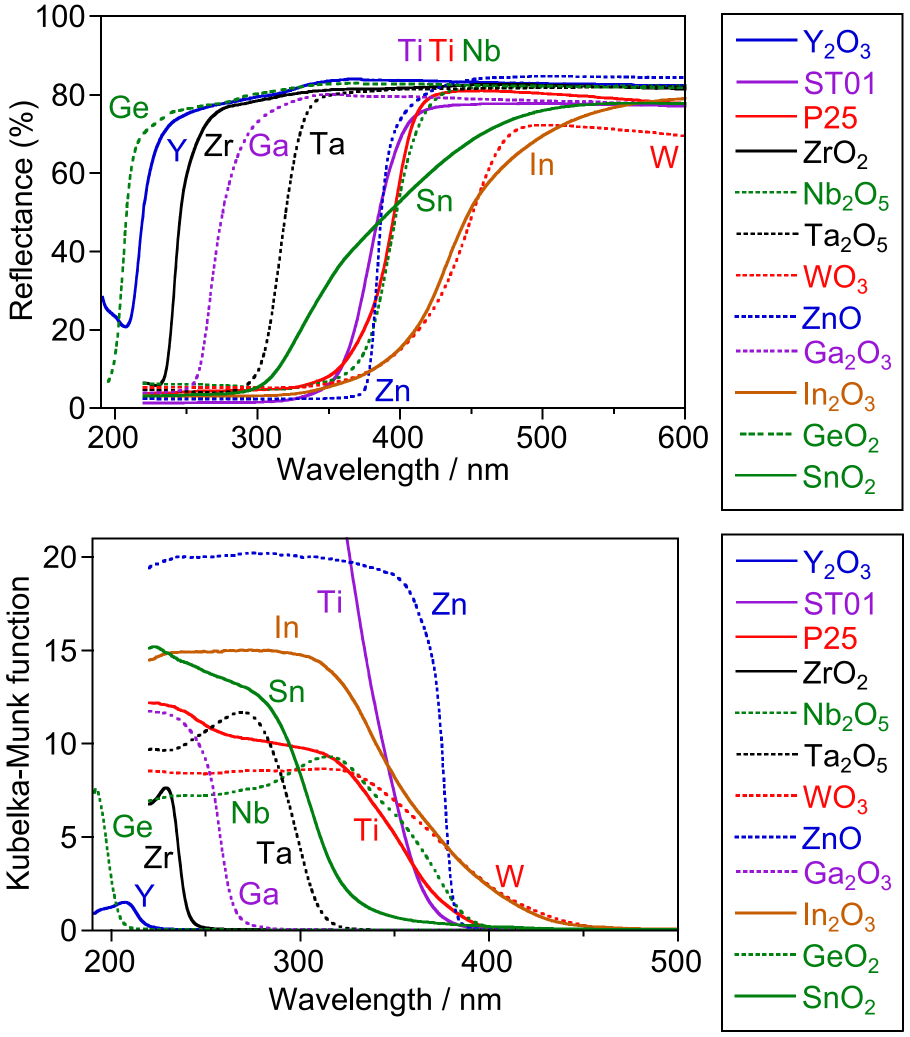

Figure S4. Diffuse reflectance UV-visible spectra of the commercial metal oxide powders. The reflectance (R) was measured with respect to $BaSO_4$. Kubelka-Munk function, $f(R)$, is converted from the R by the following equation.

$$f(R) = \frac{(1-R)^2}{2R} \tag{2}$$

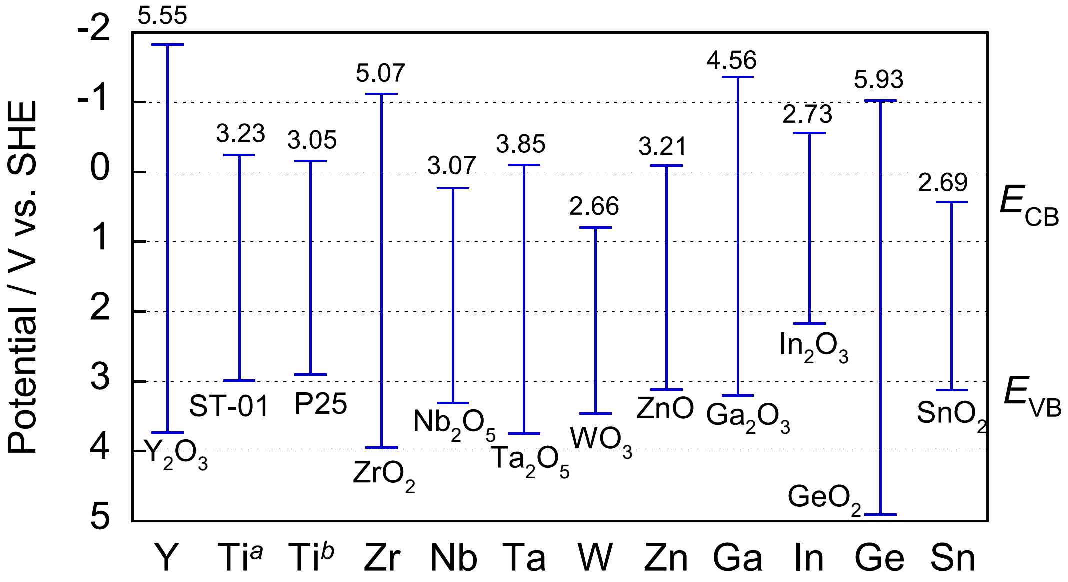

Figure S5. Bandgap (E_g) and proposed band alignment of metal oxide samples. The E_g was obtained from the diffuse reflectance UV-visible spectra. The conduction band minimum (E_{CB}) was estimated from the E_g and the electronegativity (X) of the oxide using the equation, $E_{CB} = -4.44 + X - 0.5\ E_g$. The valence band maximum (E_{VB}) was determined from the E_{CB} and the E_g.

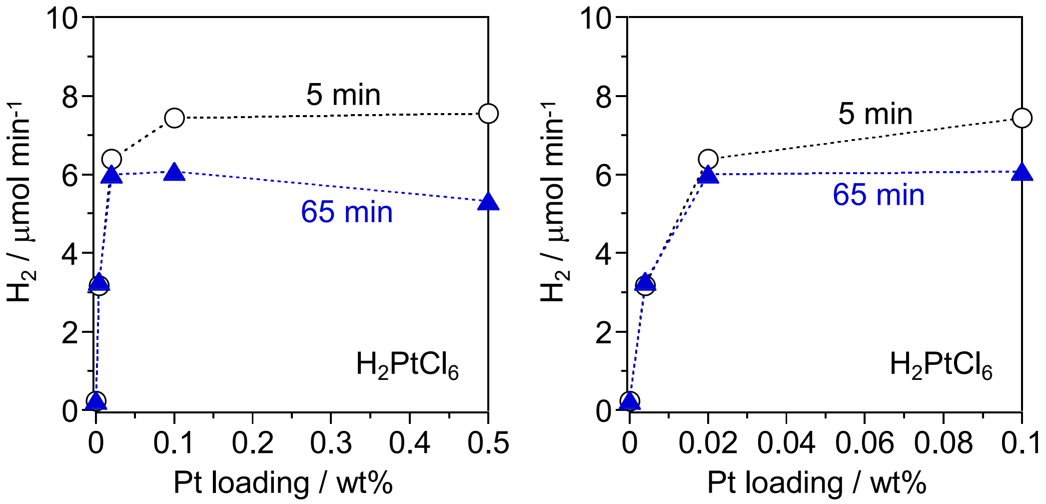

Figure S6. Effect of Pt loading on the H_2 formation rate over Pt/Ga_2O_3 (100 mg) under 254-nm UV irradiation (33 mW cm^{-2}) for 5 min and 65 min. The precursor was H_2PtCl_6. The amount of Pt loading was controlled by the concentration of the precursor solution in the IWI method. The right-side figure is the enlargement of the region of low Pt loading. The photocatalytic reaction was performed at total pressure (P_{total}) =101 kPa with $CH_4/H_2O/Ar$ = 10/3/88.

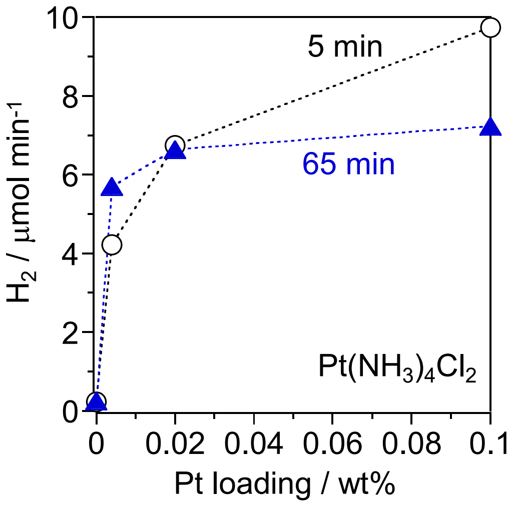

Figure S7. Effect of Pt loading on the H_2 formation rate over Pt/Ga_2O_3 (100 mg) under 254-nm UV irradiation (33 mW cm^{-2}) for 5 min and 65 min. The precursor was $Pt(NH_3)_4Cl_2$. The photocatalytic reaction was performed at P_{total} =101 kPa with $CH_4/H_2O/Ar$ = 10/3/88.

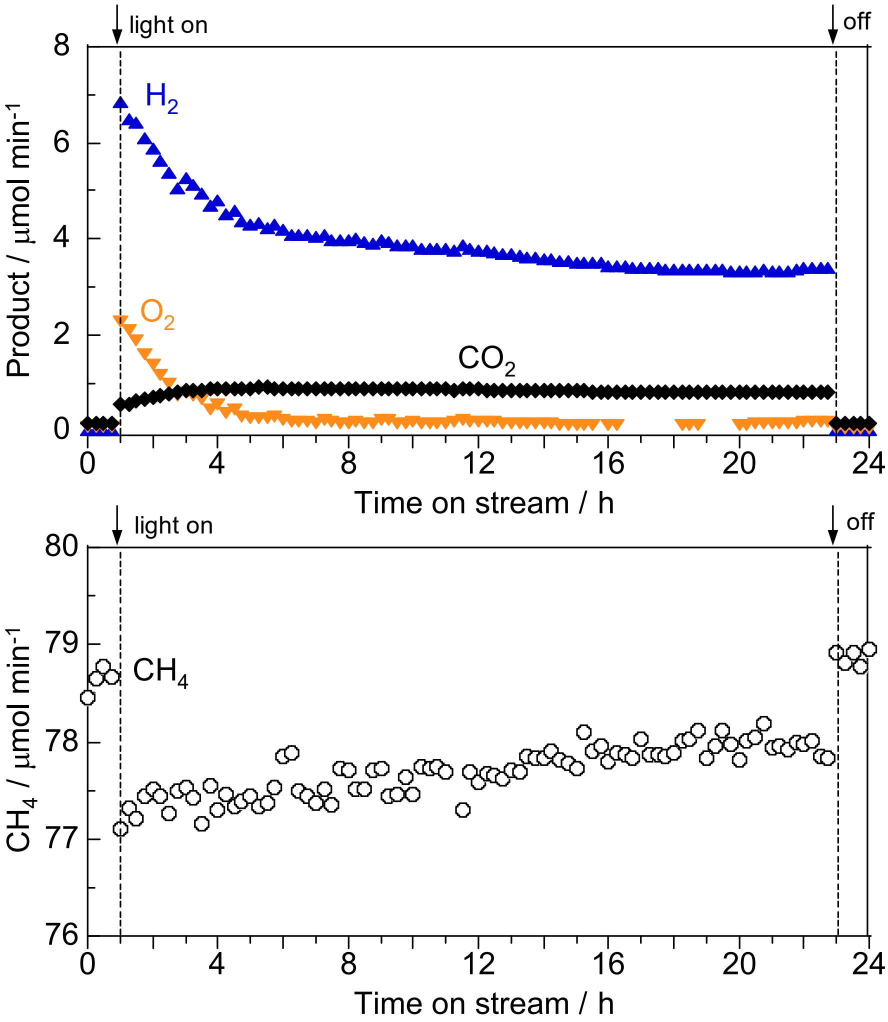

Figure S8. Time course of the production rates of H_2, O_2, and CO_2 with 0.1wt% Pt/Ga_2O_3 (100 mg) in the photocatalytic CH_4 conversion under UV light irradiation (254 nm, 33 mW cm^{-2}). Total pressure (P_{total}) =101 kPa. CH_4/H_2O/Ar = 10/3/88. Photoirradiation was performed for the long term (1–23 h time on stream).

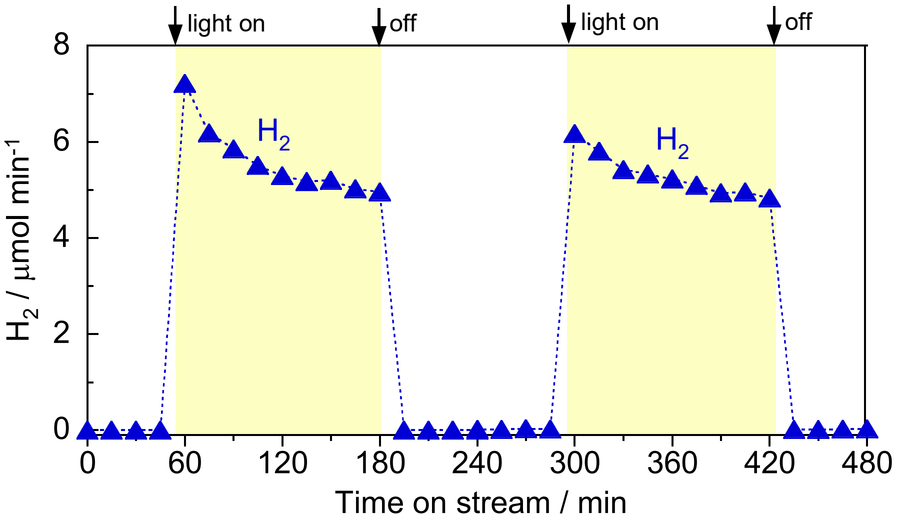

Figure S9. Time course of the production rate of H_2 with 0.02wt% Pt/Ga_2O_3 (100 mg) in the photocatalytic CH_4 conversion under UV light irradiation (254 nm, 33 mW cm^{-2}). Total pressure (P_{total}) =101 kPa. CH_4/H_2O/Ar = 10/3/88. Photoirradiation was repeatedly performed two times (60–180 and 300–420 min time on stream).

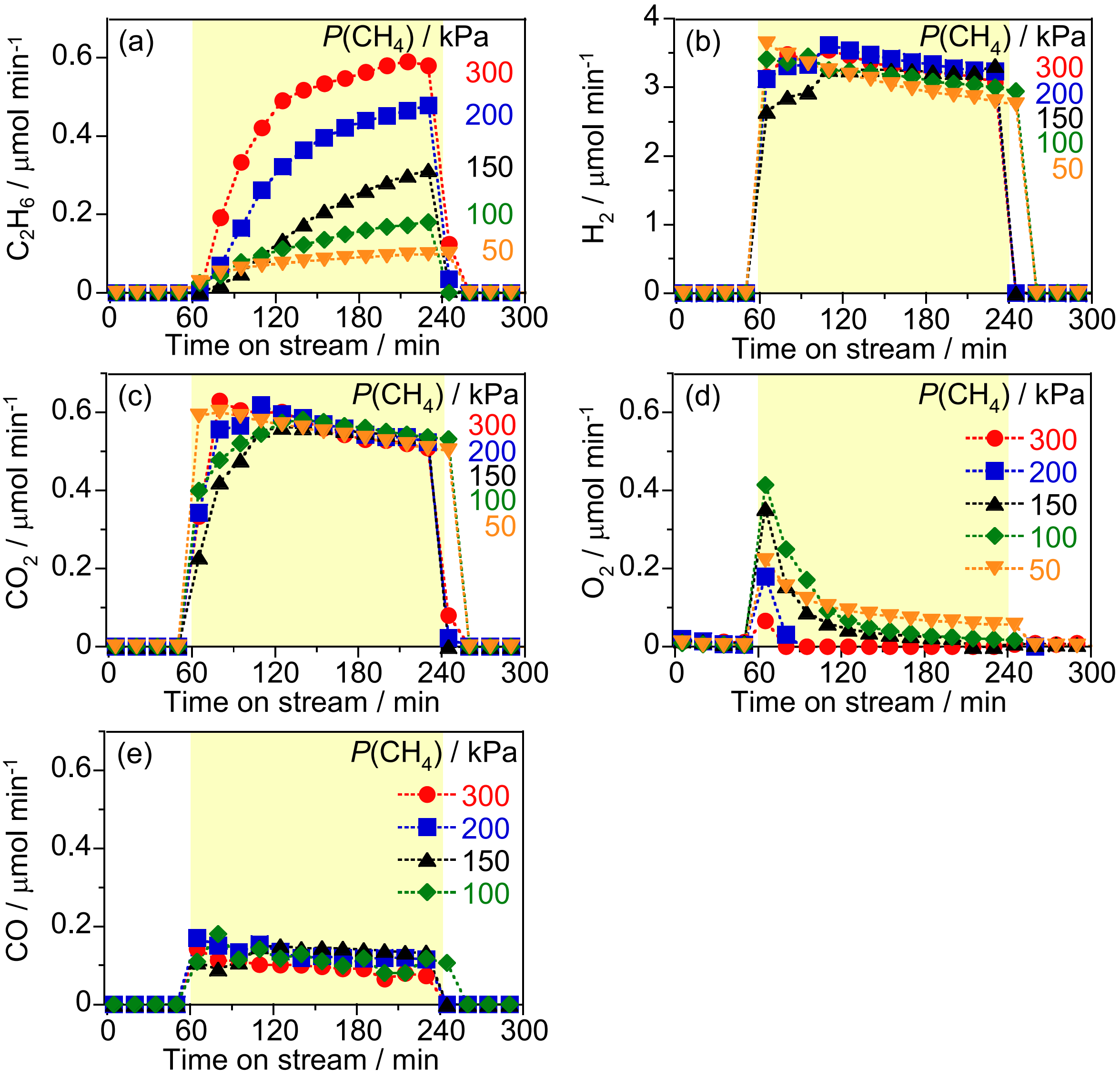

Figure S10. Time courses of the formation rate of (a) C_2H_6, (b) H_2, (c) CO_2, (d) O_2, and (e) CO over Pt/Ga_2O_3 at different pressure of CH_4, $P(CH_4)$ = 50, 100, 150, 200, and 300 kPa. $P(H_2O)$ = 3 kPa. UV light (254 nm, 15 mW cm^{-2}) was irradiated at 25 °C for 3 h (60–240 min time on stream).

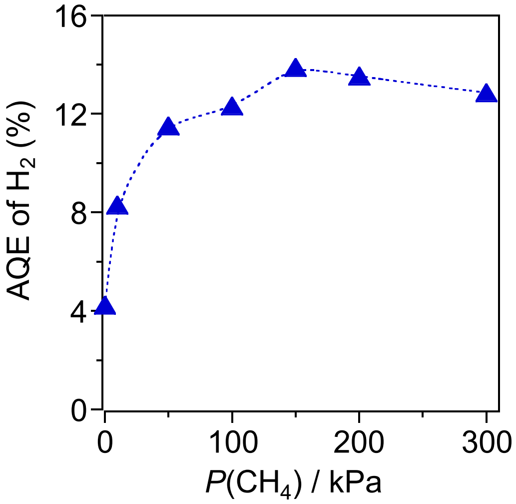

Figure S11. Effect of *P*(CH_4) on the apparent quantum efficiency (AQE) of Pt/Ga_2O_3 under 254-nm irradiation for H_2 evolution from CH_4 in the presence of H_2O (3 kPa).

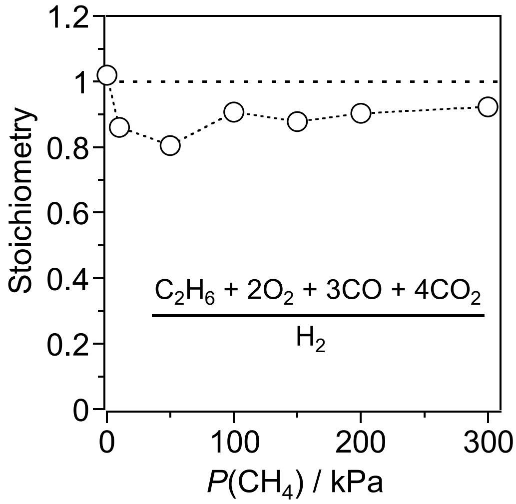

Figure S12. Effect of *P*(CH_4) on the stoichiometry of the products by Pt/Ga_2O_3 under 254-nm irradiation. Assuming dehydrogenative reactions, the production of 1 mol of C_2H_6, O_2, CO, and CO_2 is accompanied by the production of 1 mol, 2 mol, 3 mol, and 4 mol of H_2, respectively. The sum of each oxidized product multiplied by the stoichiometric coefficient should be equal to the produced H_2. The errors in the material balance were about 10% at *P*(CH_4) > 100 kPa. The deviations from the theoretical value at *P*(CH_4) = 10 and 50 kPa are because CO was not quantified in this region due to the issue in the resolution of GC analysis. The proposed schemes of dehydrogenative reactions are described as follows.

$$2CH_4 \rightarrow C_2H_6 + H_2 \qquad (3)$$

$$2H_2O \rightarrow O_2 + 2H_2 \qquad (4)$$

$$CH_4 + H_2O \rightarrow CO + 3H_2 \qquad (5)$$

$$CH_4 + 2H_2O \rightarrow CO_2 + 4H_2 \qquad (6)$$

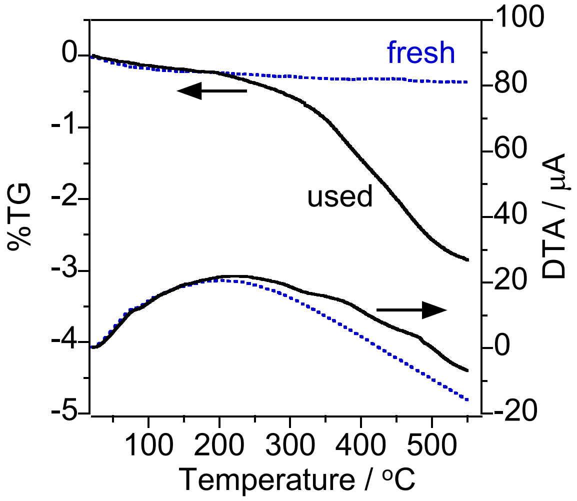

Figure S13. TG-DTA curves of 0.1 wt% Pt/Ga_2O_3 before and after the photocatalytic reaction. The dashed and solid curves show the results of the fresh and the used Pt/Ga_2O_3, respectively. The measurement was performed under air. The weight loss of the used sample associated with the exotherm suggests the formation of carbon species during the photocatalytic reaction.

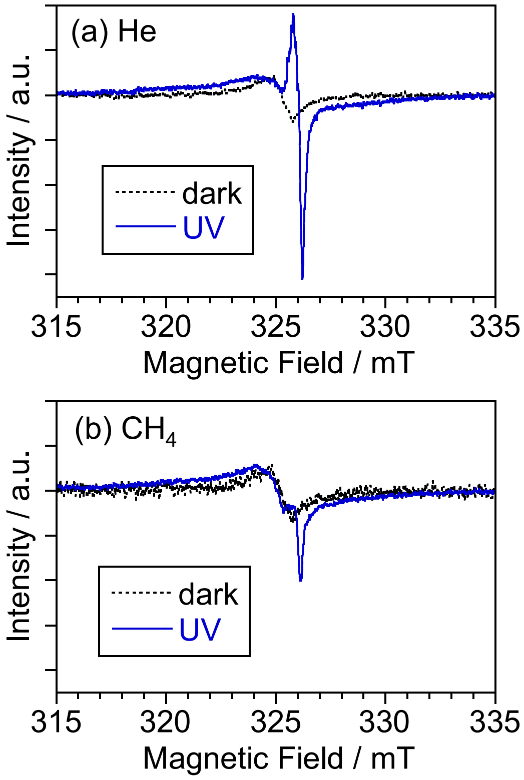

Figure S14. ESR spectra of Ga_2O_3 powder with (a) 10 kPa He and (b) 10 kPa CH_4 in a glass tube at −196 °C. The Ga_2O_3 was pretreated by evacuation at room temperature for 30 min. The dashed and solid curves show the spectra in the dark and after 248-nm UV irradiation for 1 min.

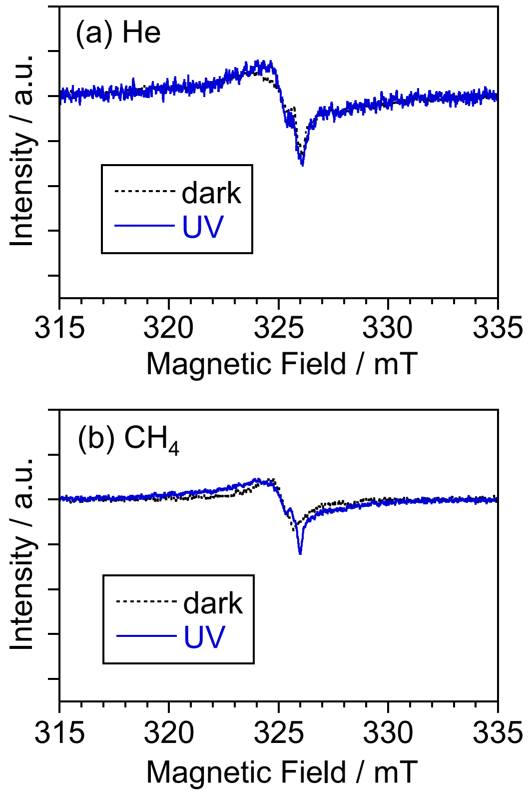

Figure S15. ESR spectra of the dehydrated Ga_2O_3 powder in (a) 10 kPa He and (b) 10 kPa CH_4 at −196 °C. The Ga_2O_3 was pretreated by evacuation at 200 °C for 30 min. The dashed and solid curves show the spectra in the dark and after 248-nm UV irradiation for 1 min.

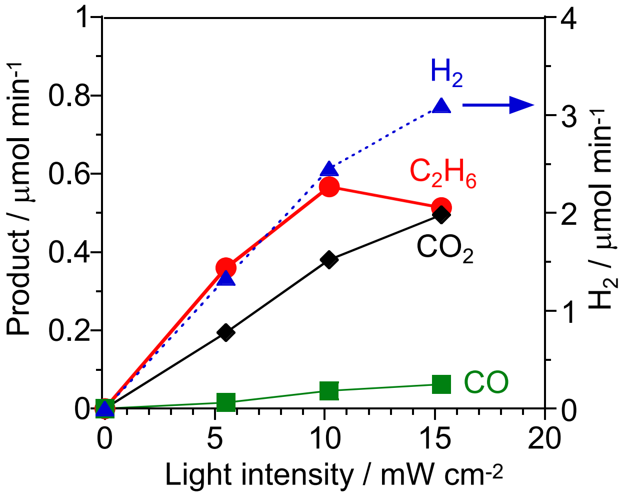

Figure S16. Effect of light intensity on the rates of product formation over 0.1 wt% Pt/Ga_2O_3. The photocatalytic reaction was performed under 254-nm UV irradiation at P_{total} of 203 kPa (CH_4/H_2O = 200/3).

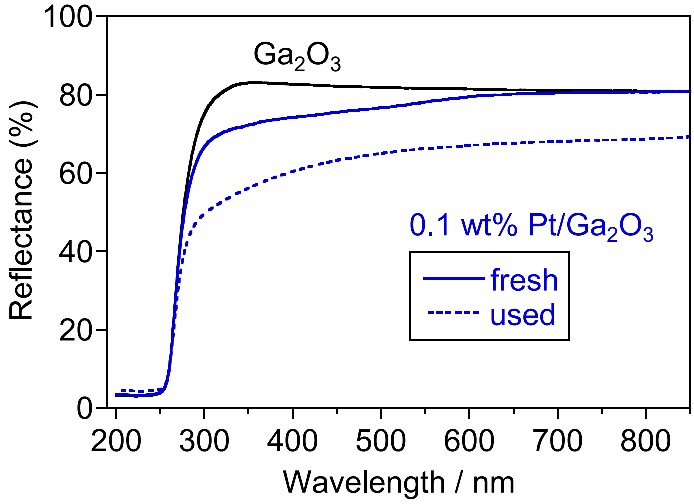

Figure S17. Diffuse reflectance UV-visible spectra of Ga_2O_3, 0.1 wt% Pt/Ga_2O_3 (fresh sample), and the 0.1 wt% Pt/Ga_2O_3 after photocatalytic reaction (used sample). The reflectance of the Pt/Ga_2O_3 was uniformly decreased at wavelengths longer than the interband transition after the photocatalytic reaction. The broad absorption of the used Pt/Ga_2O_3 suggests the formation of platinum metal nanoparticles.

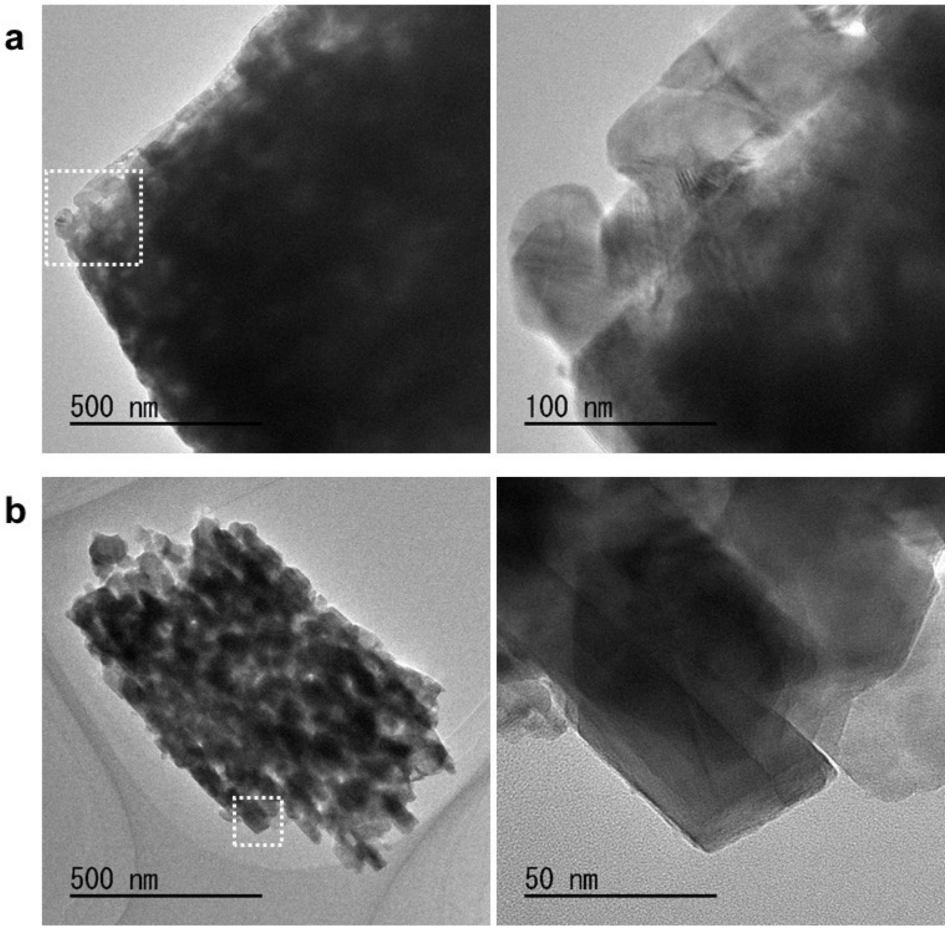

Figure S18. TEM images of (a) fresh Pt/Ga_2O_3 and (b) Pt/Ga_2O_3 after the photocatalytic CH_4 conversion. The right-side image is the enlargement of the area enclosed by the white dashed square in the left side image.